Electronic Supplementary Information

The impact of dendrite morphology on the optical properties of sunflower mimic plasmonic metasurfaces

Sunil Mehla,*[a] Sivacarendran Balendhran,[b] and Suresh K. Bhargava*[a]

S1 Experimental

S1.1 Materials and reagents

Boron-doped silicon wafers, AZ5214-E resist, and AZ400 K developer were purchased from MicroChemicals GmbH. Hydrogen tetrachloroaurate(III) trihydrate ($HAuCl_4 \cdot 3H_2O$) and lead(II) acetate tri-hydrate ($Pb(CH_3COO)_2 \cdot 3H_2O$) were purchased from Sigma-Aldrich and used as received. Milli-Q water (18.2 MU cm^{-1}) was used for all synthesis, cleaning, and testing procedures.

S1.2 Fabrication of sunflower mimic plasmonic metasurfaces

In brief, a hexagonally ordered gold disc array was first patterned on a titanium coated silicon substrate using maskless photolithography and e-beam evaporation as described in **Section S1.3**. This was followed by deposition of an insulating SiO_2 film of 50 nm thickness to obtain electrically anisotropic Au-SiO_2 disc arrays. SiO_2 deposition was performed using e-beam evaporation without any substrate rotation. This led to selective passivation of all horizontal surfaces including the substrate and the circular surfaces of gold disc arrays while the lateral surfaces of gold disc arrays were not covered and left conducting. Subsequent electrodeposition on Au-SiO_2 disc arrays as working electrodes resulted in growth of dendritic gold nanostructures only on the lateral surfaces of gold discs and gave them the shape of a gold sunflower. The two-step lateral electrodeposition method allowed good control over all geometrical aspects of the sunflower mimic metasurfaces. The diameter of Au-SiO_2 discs, their order of arrangement, and array periodicity was controlled through maskless photolithography whereas the morphology of laterally electrodeposited gold dendrites was controlled through electrodeposition. Electrodeposition of gold dendrites was performed using a custom electrolyte solution consisting of chloroauric acid, lead acetate and water as detailed in **Section S1.4**. The shape of gold dendrites was controlled through the control of chloroauric acid concentration in the electrolyte without changing the lead acetate concentration. Gold dendrites were obtained in three different shapes i.e., 2D leaf-like (GSA1), branched-conical shape where several conical dendrites grew atop and branched from the

parent cone (GSA2) and conical shape (GSA3). The length and aspect ratio of gold dendrites were controlled through the control of electrodeposition time. The three gold sunflower arrays compared in this article consisted of the same hexagonal order of arrangement, same diameter of the Au-SiO_2 disc (5 μm), and the same array pitch (1 μm). Thus, the observed differences in optical properties of the sunflower arrays originated only from the differences in morphology of the gold dendrites.

S1.3 Fabrication of Au-SiO_2 disc arrays

Surface patterns were designed using KLayout. A Kurt J. Lesker e-beam evaporator was used for the deposition of Ti, Au, and SiO_2 thin films. A 200 nm thick Ti film was first coated on a silicon wafer before surface patterning. The Ti coated Si wafers were then cleaned with water, acetone, isopropyl alcohol and O_2 plasma. AZ5214-E resist was spin-coated on the wafers at 3000 rpm for 30 seconds followed by a soft bake at 90 ^oC for 90 seconds. The resist coated wafers were exposed using maskless aligner MLA-150 using an exposure power of 25 mJ/cm^2 followed by a hard bake at 120 ^oC for 120 seconds and UV flood exposure for 17 seconds. The obtained wafers were developed using 1:4 water/AZ400K solutions for 45 seconds and washed with water to obtain a hexagonally ordered honeycomb patterned resist films. A 200 nm gold film was deposited using e-Beam evaporation and patterns were lifted-off in acetone under sonication post metallization. After lift-off well-defined gold disc arrays were obtained which were further coated with a SiO_2 film of 50 nm thickness to obtain Au-SiO_2 disc arrays. Dicing of the patterned Si wafers into sensor chips was performed using a Disco 321 machine with a diamond blade.

S1.4 Lateral electrodeposition of gold sunflower arrays

Lateral electrodeposition was performed in a three-electrode configuration using a potentiostat (CH Instruments, CHI 760C) and a custom electroplating solution consisting of chloroauric acid, lead acetate and water. The lead acetate concentration was kept constate at 1.0 mM in all the experiments. A potential difference of 0.05 V was applied against the reference electrode for different durations. Gold sunflower array with 2D leaf-like dendrites was synthesized using a chloroauric acid concentration of 3.4 mM in the electrolyte and a growth duration of 6 mins. Gold sunflower array with branched-conical dendrites were obtained from a chloroauric acid concentration of 1.7 mM in the electrolyte and a growth duration of 6 mins. Gold sunflower array with conical dendrites were obtained from a chloroauric acid concentration of 0.5 mM in the electrolyte and a growth duration of 1 min.

S1.5 Morphological characterization

Scanning electron microscopy (SEM) and energy dispersive X-ray (EDX) analysis of the samples was performed using a FEI Verios field emission scanning electron microscope. SEM images were obtained using electron beam energy of 2 kV whereas EDX analyses were obtained using electron beam energy of 30 kV. The SEM images of fabricated GSAs with different shapes of gold dendrites on the lateral surfaces are depicted in **Fig. 2a-2c**. It was clear from these SEM images that 2D leaf-like gold dendrites had the largest structures whereas conical gold dendrites had the smallest structures. The SEM images were processed using ImageJ to determine the average values of dendrite length, width, aspect ratio and packing densities from multiple measurements and these measurements are shown in **Table 1**. The EDS spectra obtained from the different GSAs is shown in **Fig. 2d**. In the EDS spectra only peaks corresponding to the presence of oxygen, silicon, gold, and titanium were observed. It was clear from Fig. 2d that leaf-like gold dendrites had the highest gold content followed by branched-conical and conical gold dendrites. The elemental maps obtained for GSA with branched-conical dendrites are shown in **Fig. 2e**.

S1.6 Evaluation of the optical properties

Spectrophotometry studies were performed using the CRAIC Apollo UV-Vis-NIR spectrophotometer in the wavelength region from 200 – 2000 nm. Eight-point calibration was performed before each measurement based on the transmission spectra of holmium oxide, didymium, and erbium for wavelength calibration and absorbance spectra of five calibration standards for intensity calibration. The reflectance spectra for gold sunflower arrays were collected from a region of 50 × 50 μm^2 from 7 different regions having an identical structure. The collected data was averaged over the data points and mean reflectance intensities and relative standard deviation (RSD) were calculated for each sample. Variation in optical response of gold sunflower microelectrode arrays were less than a relative standard deviation of 14.52 %. The reflectance data was normalized by the maximum reflectance intensity for each sample.

S1.7 Surface-enhanced Raman scattering

Different solutions with varying concentrations of 4-aminothiophenol (ATP) were prepared by first dissolving the ATP powder required for a 1 mM solution in ethanol, sonication, and dilution of the parent solution to obtain the different concentrations. Each SERS sensor chip under investigation was soaked in 2 ml aliquots taken from the freshly prepared ATP solutions for a duration of 15 minutes, rinsed with water and dried with a nitrogen gun. SERS

experiments were conducted using a Perkin Elmer Raman Station 200F (785 nm laser, spot size of 50 μm) with an exposure time of 10 seconds and 5 acquisitions per data point with no automatic background correction. The background correction was performed manually using the Perkin Elmer background correction software.

S2. FDTD Simulations

S2.1 Design of parametric models for FDTD simulations

The exact length, and width of each dendrite, their orientation in 3D space and the packing density of gold dendrites on a single sunflower unit varied between a range of values. The range of variations (±) in length, width and packing density in experimentally synthesized gold sunflower arrays are clear from Table 1. The parametric models for FDTD simulations were designed based on the structure of experimentally synthesized gold sunflower arrays. However, modelling of the effect of variations in length, width and orientation of the gold dendrites was not performed to reduce the requirements for computing resources. Similarly, in all parametric models Au-SiO_2 discs of 1 μm diameter were used instead of 5 μm for the experimentally synthesized gold sunflowers to minimize computing resources. The different variables in the parametric models are defined in section S3 of the supporting information and schematically shown in Fig. S1.

In this study a total of 10 parametric models (PM0 – PM9) were designed and simulated as summarized in Fig. 3. Model PM0 was equivalent to GSA0 and represented an Au-SiO_2 disc array. Models PM1, PM2, and PM3 represented GSAs with leaf-like dendrites and a constant packing density of 12 but aspect ratios of 2.5, 1.25, and 0.5, respectively. A packing density of 12 was used because of the large width of leaf-like dendrites compared to other models. Models PM4, PM5, and PM6 represented GSAs with conical dendrites and a constant packing density of 24 but aspect ratios of 5, 2.5, and 1, respectively. A packing density of 24 was used in these models because conical dendrites had the lowest width compared to other models. Model PM7 consisted of the same length, width, and aspect ratio of leaf-like gold dendrites as PM2 but a higher packing density of 24. Similarly, model PM8 consisted of the same length, width, and aspect ratio of conical gold dendrites as model PM5 but a higher packing density of 48. Model PM9 represented GSA with branched-conical dendrites with a packing density of 24.

S2.2 FDTD simulations

Electric filed simulations were obtained using the finite difference time domain method (FDTD) and performed with a commercial package (Lumerical FDTD Solutions, 2021). A plane wave source (0.2-2 μm) polarized in the Y direction was used at normal incidence. Periodic boundary conditions were

used for the X- and Y-direction boundaries. In all the parametric models the diameter of the Au-SiO_2 disc was 1 μm, the centre-to-centre separation between two nearest sunflowers was 2 μm which corresponded to an array pitch of 1 μm. Perfectly matched layer (PML) boundaries were used in the Z-direction, which allowed simulation of the free space above the gold sunflower arrays and below the bottom titanium coated silicon substrate. The frequency dependent complex refractive index of SiO_2, Si, Ti, Ni, and Au were obtained from Palik. A uniform grid with a mesh size of 10 nm was used for the FDTD simulations.

S3. Definitions of variables in the parametric models

Spatial orientation of gold dendrites: The orientation of a gold dendrite in 3D space was defined in the polar coordinates (r, θ, φ) as shown in Fig. S1a, where r was the distance of the dendrite's center of mass from the center of its gold sunflower unit, θ was the angular coordinate in the Z direction and φ was the angular coordinate in the XY plane. To minimize computational load for the FDTD simulations, the angular coordinate θ was kept 0 in all the models implying that all the dendrites were horizontally oriented in the XY plane in the designed parametric models. The angular coordinates ϕ_l, $\phi_{b\text{-}c}$ *and* ϕ_c for gold sunflower arrays with leaf-like, branched-conical, and conical dendrites, respectively, are depicted in Fig. S1b-S1e. For all gold sunflower arrays, the angular separation between each dendrite on the lateral surface was kept equal such that the angular coordinate φ satisfied the relation, $\phi = 2\pi/n$, where the variable n was the number of gold dendrites present on the lateral surface of a gold sunflower. For gold sunflower arrays with branched-conical dendrites several smaller cones branched out from the parent cone. In the designed parametric models, the spatial orientation of these small cones which were attached to the parent cone is depicted in Fig. S1d. A constant angular separation (α_2) of 120° in the XY plane was used in the simulations between the three smaller cones of length l_1 and the three larger cones of length l_2. A fixed angular separation (α_1) of 60° was used in the simulations between the smaller and larger cones as shown in Fig. S1d.

Packing density: The packing density for gold sunflower arrays was defined as the number of dendrites present on the lateral surfaces of one gold sunflower unit. The packing densities n_l, $n_{b\text{-}c}$, and n_c for gold sunflower arrays containing leaf-like, branched-conical, and conical dendrites, respectively, are shown in Fig. S1b-S1e.

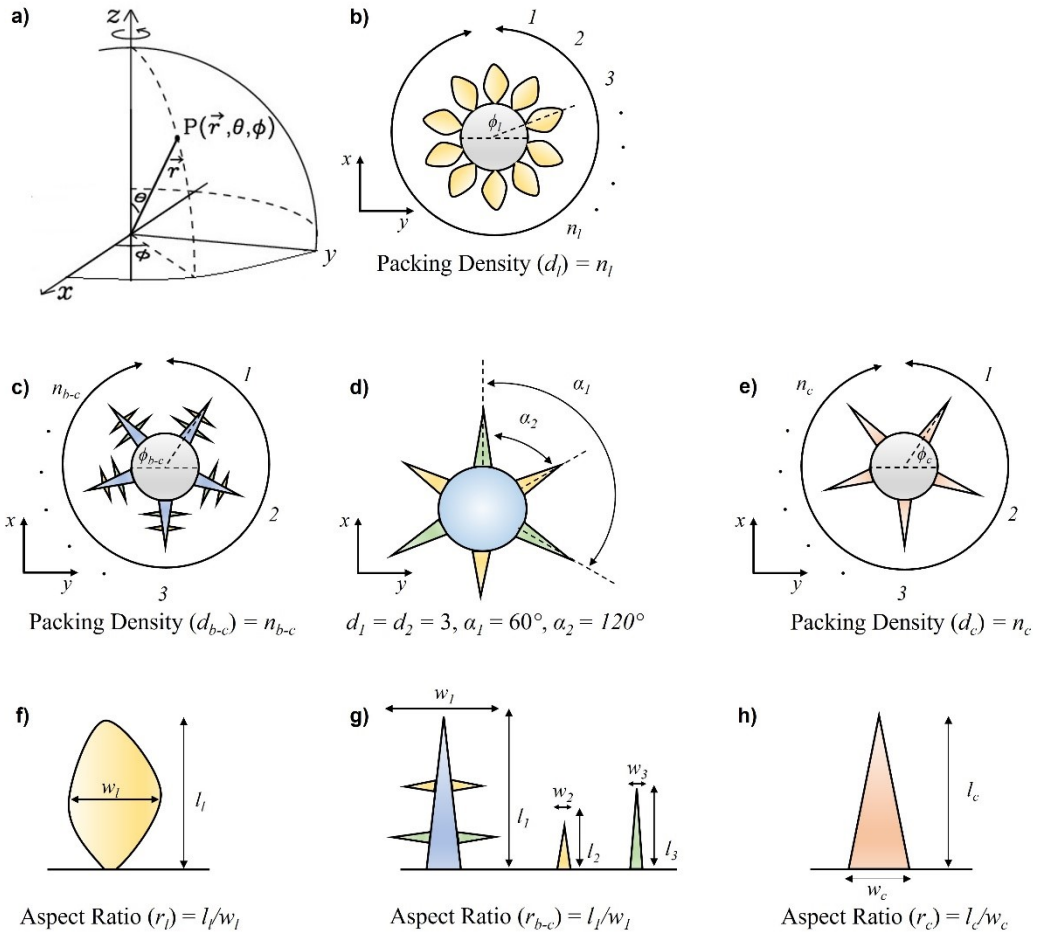

Fig. S1. Definition of different parameters used in the design of sunflower mimic parametric models for FDTD simulations: a) representation of a gold dendrite as a point (P) in 3D space and its location in polar coordinates, b) packing density (d_l), c) packing density ($d_{b\text{-}c}$), d) packing densities d_1, and d_2 and orientation angles α_1 and α_2, e) packing density (d_c), f) aspect ratio (r_l), g) aspect ratio ($r_{b\text{-}c}$, r_2 and r_3), and h) aspect ratio (r_c).

Dendrite length, width, and aspect ratio: In the designed parametric models for FDTD simulations, leaf-like dendrites were designed in the shape of 2D leaves as depicted in Fig. S1f. The length (l_l) of a leaf-like dendrite was the vertical distance between the base and the vertex of the dendrite. The width (w_l) of a leaf-like dendrite was the span of the dendrite at a height where the width was maximum as shown in Fig. S1f. Aspect ratio (r_l) was calculated as the ratio of length to width ($r_l = l_l/w_l$).

The branched-conical dendrites in the parametric models consisted of one parent cone, 3 small cones and 3 large cones as depicted in Fig. S1d and S1g. The lengths l_1, l_2, *and* l_3 in branched-conical dendrites were the vertical distance between the base and the vertex of the parent cone, small cones, and large cones, respectively. The width w_1 for the branched-conical dendrite was defined as the maximum width of the dendrite i.e., extending from the vertex of a large cone on one side to the vertex of a large cone on the other side as shown in Fig. S1g. The widths w_2, *and* w_3 in branched-conical

dendrites were defined as the width of the conical base of the small cones, and large cones, respectively. Correspondingly, three aspect ratios can be calculated from the ratio of lengths to widths (r_1=l_1/w_1, r_2=l_2/w_2, and r_3 = l_3/w_3). However, in this article discussions were made only on the basis of the aspect ratio of the parent cone of the branched conical dendrites i.e., $r_{b\text{-}c} = r_1 = l_1/w_1$

The length (l_c) of a conical dendrite was the vertical distance between the base and the vertex of the dendrite. The width (w_c) of a conical dendrite was the width of the dendrite at the base of the cone as shown in Fig. S1h. Aspect ratio (r_c) was calculated as the ratio of length to width ($r_c = l_c/w_c$).

S4. Calculation of SERS Enhancement Factors

SERS enhancement factors (EF) were calculated on the basis of SERS enhancements obtained for gold sunflowers in comparison to a flat substrate consisting of a 200 nm thick gold layer on a silicon substrate as a reference sample. The SERS intensity of the a_1 peak at 1078 cm^{-1} was used for EF calculation. The SERS spectra for gold sunflowers were obtained from a 1 µM ATP solution. SERS enhancement was not observed for flat gold substrate when 1 µM ATP solution was used. For the flat gold substrate some SERS enhancement was observed when a 0.1 M ATP solution was used. Enhancement factor was calculated as:

$$\mathrm{EF} = \frac{Is \times Co}{Io \times Cs}$$

where

Is: Intensity at 1078 cm^{-1} obtained from SERS spectrum of a sample

Cs: Concentration of 4-aminothiophenol used to obtain the SERS spectra of the sample

Io: Intensity at 1078 cm^{-1} obtained from SERS spectrum of the reference sample

Co: Concentration of 4-aminothiophenol used to obtain the SERS spectra of reference sample

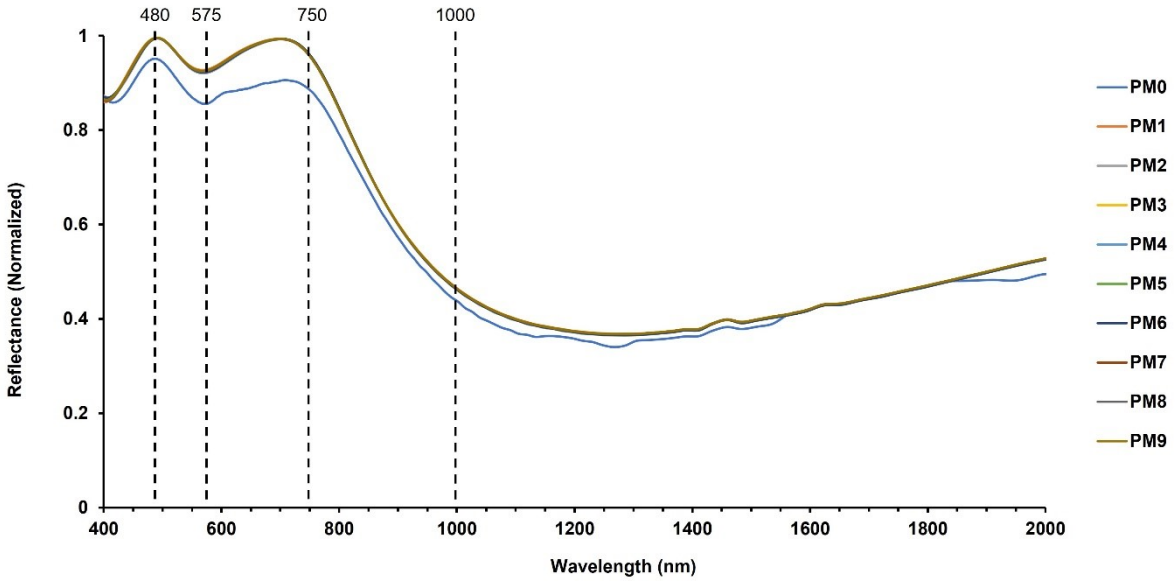

Fig. S2 Simulated reflectance spectra obtained from the designed sunflower mimic parametric models (PM0 – PM9) in the wavelength region from 400 – 2000 nm. The electric field intensity distributions in the XY and XZ planes were simulated only for selective wavelengths of 480, 575, 750 and 1000 nm.

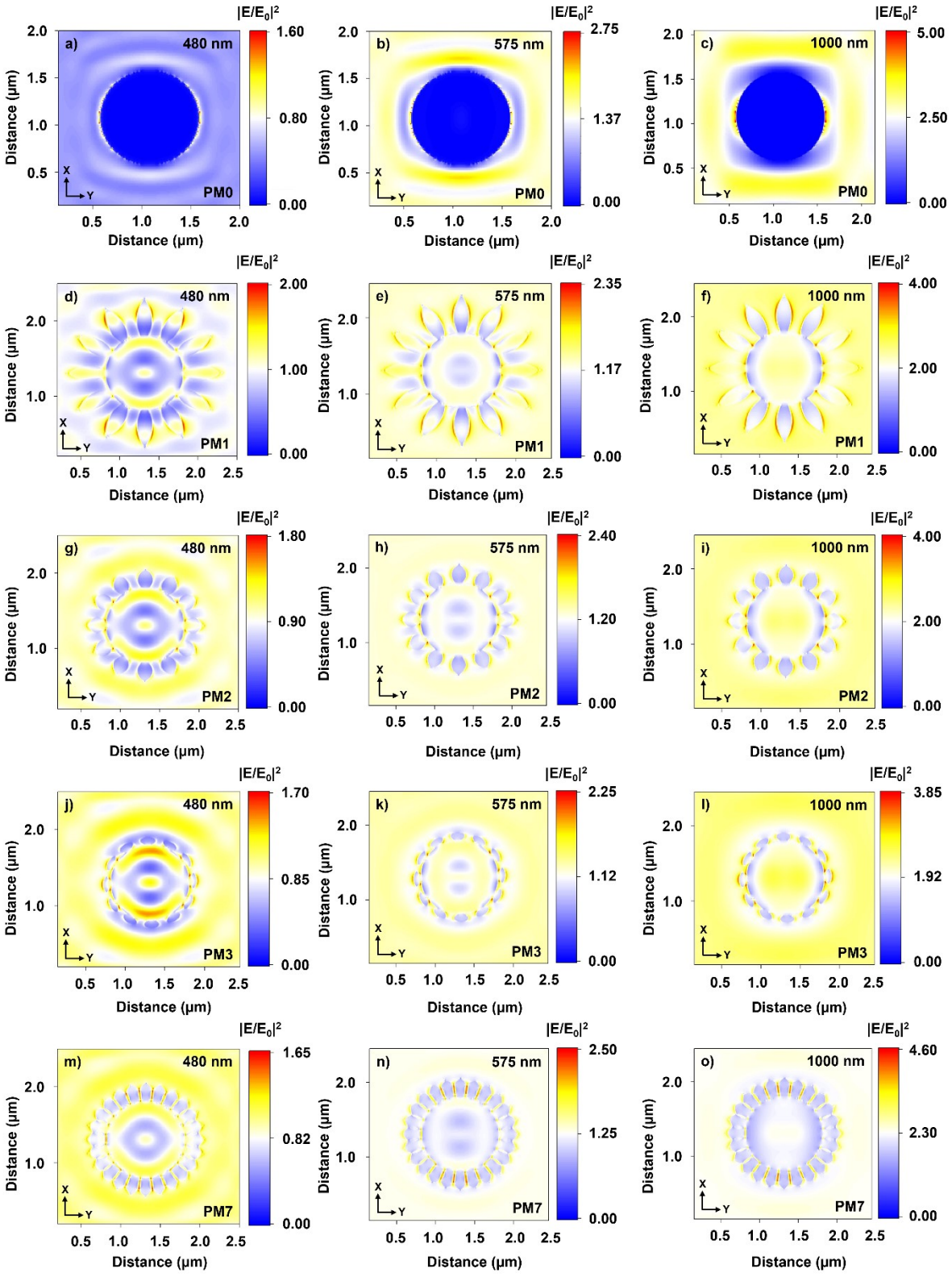

Fig. S3 Distribution of the squared normalized electric field intensities and hot spots in the XY plane passing through the middle of the gold dendrites in parametric models PM0, PM1, PM2, PM3 and PM7

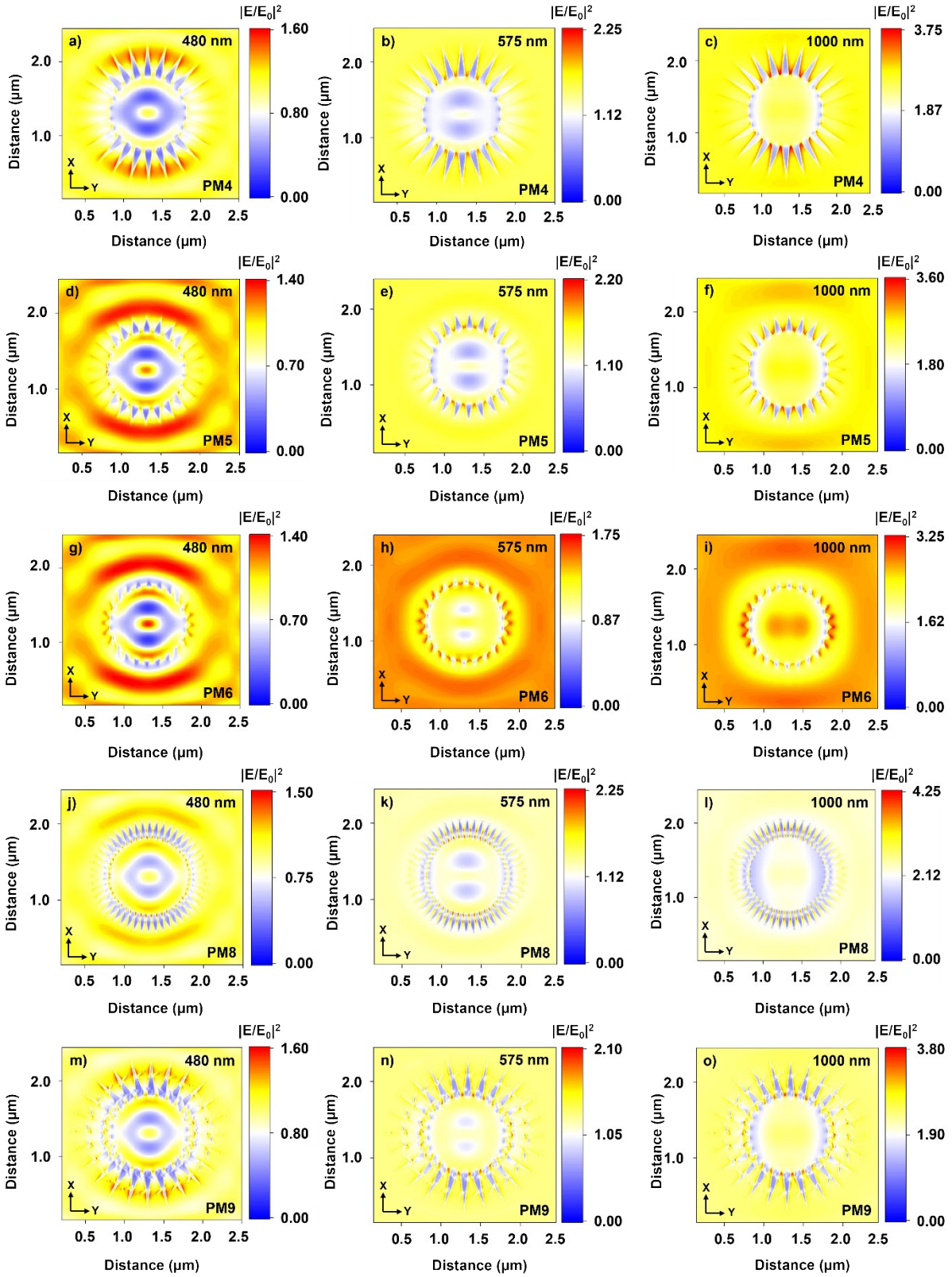

Fig. S4 Distribution of the squared normalized electric field intensities and hot spots in the XY plane passing through the middle of the gold dendrites in parametric models PM4, PM5, PM6, PM8 and PM9.

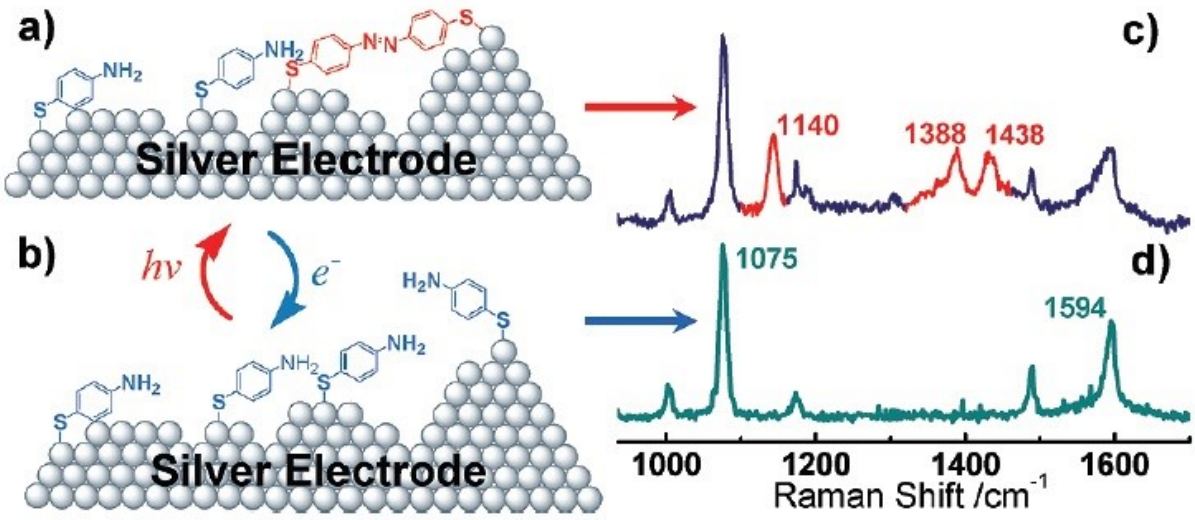

Fig. S5 Schematic illustration of the in situ photocatalytic dimerization of ATP adsorbed on a silver electrode into DMAB: a) generation of DMAB on a silver electrode by photon absorption, b) silver electrode with adsorbed ATM molecules, SERS spectrum obtained from silver electrode with adsorbed ATP and DMAB, and d) SERS spectrum obtained from silver electrode with adsorbed ATP molecules. Adapted from Journal of American Chemical Society 132, 9244-9246 (2010) with permission from the American Chemical Society, copyright © 2010